

Study of the rare decay $K^\pm \rightarrow \pi^\pm \gamma\gamma$

Cristina Lazzeroni* for the NA62 Collaboration[†]

School of Physics and Astronomy

University of Birmingham, Birmingham B15 2TT, UK

E-mail: cristina.lazzeroni@cern.ch

A new measurement of the decay $K^\pm \rightarrow \pi^\pm \gamma\gamma$ at the NA48/2 and NA62 experiments is presented. A sample of about 300 candidates has been collected during low intensity runs with minimum bias trigger configuration. The measurements of the decay spectrum and rate are presented. The decay provides further tests of the Chiral Perturbation Theory.

2013 Kaon Physics International Conference,

29 April-1 May 2013

University of Michigan, Ann Arbor, Michigan - USA

*Speaker.

[†]F. Ambrosino, A. Antonelli, G. Anzivino, R. Arcidiacono, W. Baldini, S. Balev, S. Bifani, C. Biino, A. Bizzeti, B. Bloch-Devau, V. Bolotov, F. Bucci, A. Ceccucci, P. Cenci, C. Cerri, G. Collazuol, F. Costantini, A. Cotta Ramusino, D. Coward, G. D'Agostini, P. Dalpiaz, H. Danielsson, G. Dellacasa, D. Di Filippo, L. DiLella, N. Doble, V. Duk, J. Engelfried, K. Eppard, V. Falaleev, R. Fantechi, M. Fiorini, P.L. Frabetti, A. Fucci, S. Gallorini, L. Gatignon, E. Gersabeck, A. Gianoli, S. Giudici, E. Goudzovski, S. Goy Lopez, E. Gushchin, B. Hallgren, M. Hita-Hochgesand, E. Iacopini, E. Imbergamo, V. Kekelidze, K. Kleinknecht, V. Kozhuharov, V. Kurshetsov, G. Lamanna, C. Lazzeroni, M. Lenti, E. Leonardi, L. Litov, D. Madigozhin, A. Maier, I. Mannelli, F. Marchetto, P. Massarotti, M. Misheva, N. Molokanova, M. Moulson, S. Movchan, M. Napolitano, A. Norton, T. Numao, V. Obraztsov, V. Palladino, M. Pepe, A. Peters, F. Petrucci, B. Peyaud, R. Piandani, M. Piccini, G. Pierazzini, I. Popov, Yu. Potrebenikov, M. Raggi, B. Renk, F. Retière, P. Riedler, A. Romano, P. Rubin, G. Ruggiero, A. Salamon, G. Saracino, M. Savrié, V. Semenov, A. Sergi, M. Serra, S. Shkarovskiy, M. Sozzi, T. Spadaro, P. Valente, M. Veltri, S. Venditti, H. Wahl, R. Wanke, A. Winhart, R. Winston, O. Yushchenko, A. Zinchenko.

1. Introduction

In 2003-04, the NA48/2 experiment has collected at the CERN SPS the world largest sample of charged kaon decays, with the main goal of searching for direct CP violation [1]. In 2007-08, the NA62 experiment (R_K phase) collected a large minimum bias data sample with the same detector but modified data taking conditions, with the main goal of measuring the ratio of the rates of leptonic kaon decays [2]. The large statistics accumulated by both experiments has allowed the studies of a range of rare kaon decay modes. The study of the rare decay $K^\pm \rightarrow \pi^\pm \gamma\gamma$ is presented here.

Measurements of radiative non-leptonic kaon decays provide crucial tests for the ability of the Chiral Perturbation Theory (ChPT) to explain weak low energy processes. In the ChPT framework, the $K^\pm \rightarrow \pi^\pm \gamma\gamma$ decay receives two non-interfering contributions at lowest non-trivial order $O(p^4)$: the pion and kaon loop amplitude depending on an unknown $O(1)$ parameter \hat{c} [3]. Higher order unitarity corrections from $K \rightarrow 3\pi$ decays, including the main $O(p^6)$ contribution as well as those beyond $O(p^6)$ due to using the phenomenological values of $K \rightarrow 3\pi$ amplitudes, have been found to modify the decay spectrum significantly; in particular, they lead to non-zero differential decay rate at zero di-photon invariant mass [4]. The total branching fraction is predicted to be $\sim 10^{-6}$, with the pole amplitude contributing 5% or less [4, 5]. The ChPT predictions for the decay spectra for several values of \hat{c} are presented in Fig. 1: the di-photon mass spectra exhibit a characteristic cusp at twice the pion mass due to the dominant pion loop amplitude.

Experimentally, the only published $K^\pm \rightarrow \pi^\pm \gamma\gamma$ observation is that by the BNL E787 experiment [6], of 31 decay candidates in the kinematic region $100 \text{ MeV}/c < p_\pi < 180 \text{ MeV}/c$ (where p_π is the π^+ momentum in the K^+ frame), with 5 expected background events. The measured branching fraction is $(1.10 \pm 0.32) \times 10^{-6}$ and the parameter \hat{c} is 1.6 ± 0.6 at $O(p^4)$ and 1.8 ± 0.6 at $O(p^6)$.

2. Beam, detectors and event selection

The beam line has been designed to deliver simultaneous, narrow momentum band K^+ and K^- beams derived from the primary 400 GeV/c protons extracted from the CERN SPS impinging on a beryllium target. Beam momenta of $60 \pm 3 \text{ GeV}/c$ and $74 \pm 1.5 \text{ GeV}/c$ were selected by two systems of dipole magnets, focusing quadrupoles, muon sweepers and collimators. The beam kaons decayed in a fiducial decay volume contained in a 114 m long cylindrical vacuum tank. A detailed description of the detector used in 2003-08 is available in [7]. The momenta of charged decay products are measured in a magnetic spectrometer, housed in a tank filled with helium and placed after the decay volume. The spectrometer comprises four drift chambers (DCHs), two upstream and two downstream of a dipole magnet which gives a horizontal transverse momentum kick of 120 MeV/c (NA48) or 265 MeV/c (NA62) to singly-charged particles. Each DCH is composed of eight planes of sense wires. A plastic scintillator hodoscope (HOD) producing fast trigger signals and providing precise time measurements of charged particles is placed after the spectrometer. A 27 radiation length liquid krypton (LKr) electromagnetic calorimeter located further downstream is used for lepton identification and as a photon detector. Its readout cells have a transverse size of approximately $2 \times 2 \text{ cm}^2$ each, without longitudinal segmentation.

Data for this analysis were collected during a 3-day special NA48/2 run in 2004, and a 3-month NA62 run in 2007. The latter sample has been collected with a set of downscaled trigger conditions with an effective downscaling factor of about 20. The effective kaon fluxes collected in 2004 and 2007 are similar, but the background conditions and resolution on kinematic variables differ significantly. A crucial advantage of minimum bias samples exploited by the present analyses is the absence of sizeable systematic effects due to trigger inefficiencies. The resulting total sample is about 10 times larger than the BNL E787 one.

The kaon decay vertex is reconstructed as the point of closest approach (CDA) of the track extrapolated upstream (taking into account the measured stray magnetic field in the vacuum tank) and the axis of the kaon beam of the corresponding charge (determined with fully reconstructed $K^\pm \rightarrow 3\pi$ decays). Signal events are selected requiring: only one good quality track in the detector acceptance, with momentum in the range $10(8) \text{ GeV}/c < p < 40(50) \text{ GeV}/c$ for the 2004 (2007) data, to reduce background from $K^\pm \rightarrow \pi^\pm \pi^0 \pi^0$; two isolated clusters in the LKr calorimeter with energy above 3 GeV, and in time with the reconstructed track; CDA of the track to the beam axis required to be less than 3.5 cm; reconstructed kaon decay vertex located within the decay volume (92 m long). A charged pion is identified by the ratio E/p of energy deposition in the LKr calorimeter to momentum measured by the spectrometer, which is required to be $E/p < 0.85$; this removes the background from the $K^\pm \rightarrow \pi^0 e^\pm \nu$ decay with internal or external bremsstrahlung, as well as from the structure-dependent $K^\pm \rightarrow \pi^0 e^\pm \nu \gamma$ decay. The reconstructed total and transverse momentum of the $\pi^\pm \gamma\gamma$ system with respect to the beam trajectory should be in agreement with the beam properties. The reconstructed $\pi^\pm \gamma\gamma$ invariant mass should be in the range (0.48; 0.51) GeV/c^2 . Finally, signal events are selected in the region $z = (m_{\gamma\gamma}/m_K)^2 > 0.2$ to reject the $K^\pm \rightarrow \pi^\pm \pi^0$ background peaking at $z = 0.075$.

3. Results and discussion

The $\pi^\pm \gamma\gamma$ mass distributions from data are shown in Fig. 2, together with the MC simulation expectations of the signal and background contributions. The small excess visible around 0.55 MeV is due to a special $K^\pm \rightarrow \pi^\pm \pi^0 \gamma$ background topology with photon conversion where the radiative photon is undetected, while a photon from the π^0 decay converts in the spectrometer between the first plane and the magnet, resulting in two calorimeter clusters but no reconstructed tracks; the other photon from the π^0 decay either forms a merged cluster or is outside the calorimeter acceptance. The difference between the right and left plots is due to a difference by a factor of 2 in the magnetic field integral in the spectrometer.

A total of 147 (175) decays candidates are observed in the 2004 (2007) data set, with backgrounds contaminations of about 11.6% (6.9%) from $K^\pm \rightarrow \pi^\pm \pi^0 (\pi^0) (\gamma)$ decays with merged photon clusters in the LKr calorimeter. Due to the $K^\pm \rightarrow \pi^\pm \pi^0$ background peaking at $z = 0.075$, the data are not sensitive to the region close to zero di-photon invariant mass. The data distributions of the z kinematic variable, together with the signal (at $O(p^6)$) and background expectations, are displayed in Fig. 3: they support the ChPT expectation of a cusp at the two-pion threshold. The values of the \hat{c} parameter have been measured in the framework of the ChPT $O(p^4)$ and $O(p^6)$ parameterization (according to [4]) by performing log-likelihood fits to the data. The preliminary results of the fits are in agreement with the earlier BNL E787 ones. The uncertainties are domi-

nated by the statistical one; the systematic errors are mainly due to uncertainties in the background estimates. The $O(p^6)$ parametrization involves a number of external inputs, fixed as follows: the polynomial contribution terms are $\eta_1 = 2.06$, $\eta_2 = 0.24$ and $\eta_3 = -0.26$ as suggested in [4], while the $K^\pm \rightarrow 3\pi^\pm$ amplitude parameters come from a fit to the experimental data [8]. Along with the separate 2004 and 2007 results, the combined results are presented in Table 1. The combination takes into account the large positive correlation of the systematic uncertainties of the two measurements: for $O(p^4)$ fit $\hat{c} = 1.56 \pm 0.23$; for $O(p^6)$ fit $\hat{c} = 2.00 \pm 0.26$; for $O(p^6)$ fit the branching fraction is $(1.01 \pm 0.06) \times 10^{-6}$. The $K^\pm \rightarrow \pi^\pm \gamma\gamma$ branching fraction as a function of \hat{c} is shown in Fig. 4 (left); differential rate in terms of $z = (m_{\gamma\gamma}/m_K)^2$, for $O(p^4)$ and $O(p^6)$ parameterizations according to [4], with \hat{c} as measured from the fit to the data, is shown in Fig. 4 (right). Data are consistent with both $O(p^4)$ and $O(p^6)$ descriptions.

	2004 data	2007 data	Combined
\hat{c} , $O(p^4)$ fit	$1.36 \pm 0.33_{stat} \pm 0.07_{syst}$	$1.71 \pm 0.29_{stat} \pm 0.06_{syst}$	$1.56 \pm 0.22_{stat} \pm 0.07_{syst}$
\hat{c} , $O(p^6)$ fit	$1.67 \pm 0.39_{stat} \pm 0.09_{syst}$	$2.21 \pm 0.31_{stat} \pm 0.08_{syst}$	$2.00 \pm 0.24_{stat} \pm 0.09_{syst}$
BR, $O(p^6)$ fit	$(0.94 \pm 0.08) \times 10^{-6}$	$(1.06 \pm 0.07) \times 10^{-6}$	$(1.01 \pm 0.06) \times 10^{-6}$

Table 1: Preliminary results of the fits to the di-photon mass distribution of $K^\pm \rightarrow \pi^\pm \gamma\gamma$ decays, with the ChPT parameterizations described in [4]. The quoted branching fraction values correspond to the full kinematic range. The combination takes into account the large positive correlation of the systematic uncertainties of the 2004 and 2007 measurements.

4. Conclusions

NA48/2 and NA62 experiments have performed new, preliminary measurements of the $K^\pm \rightarrow \pi^\pm \gamma\gamma$ decay. The achieved precision for branching fraction and form factor parameters represents a significant improvement with respect to that of the only measurement published to date. The measurements increase the precision of ChPT tests with this channel. The publication of the final result is in preparation.

References

- [1] R. Batley et al., Eur. Phys. J C52 (2007) 875.
- [2] C. Lazzeroni et al., Phys. Lett. B719 (2013) 326–336.
- [3] G. Ecker, A. Pich and E. de Rafael, Nucl. Phys. B303 (1988) 665.
- [4] G. D Ambrosio and J. Portolés, Phys. Lett. B386 (1996) 403.
- [5] J.-M. Gerard, C. Smith and S. Trine, Nucl. Phys. B730 (2005) 1.
- [6] P. Kitching et al., Phys. Rev. Lett. 79 (1997) 4079.
- [7] V. Fanti et al., Nucl. Instrum. Methods A574 (2007) 433.
- [8] J. Bijnens, P. Dhonte and F. Persson, Nucl. Phys. B648 (2003) 317.

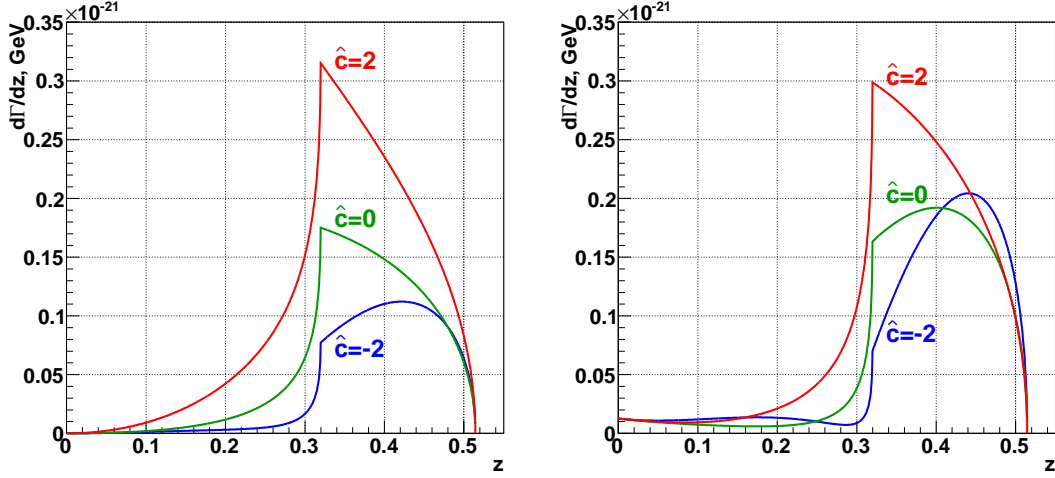


Figure 1: ChPT predictions for the $K^\pm \rightarrow \pi^\pm \gamma\gamma$ differential rate in terms of $z = (m_{\gamma\gamma}/m_K)^2$ for $O(p^4)$ (left) and $O(p^6)$ (right) parameterizations according to [4], with $\hat{c} = -2; 0; 2$. The \hat{c} -independent pole contribution is also shown. For the $O(p^6)$ parameterization, values of polynomial contributions η_i are taken from [4], and the $K^\pm \rightarrow 3\pi^\pm$ amplitude parameters are taken from a fit to experimental data [8].

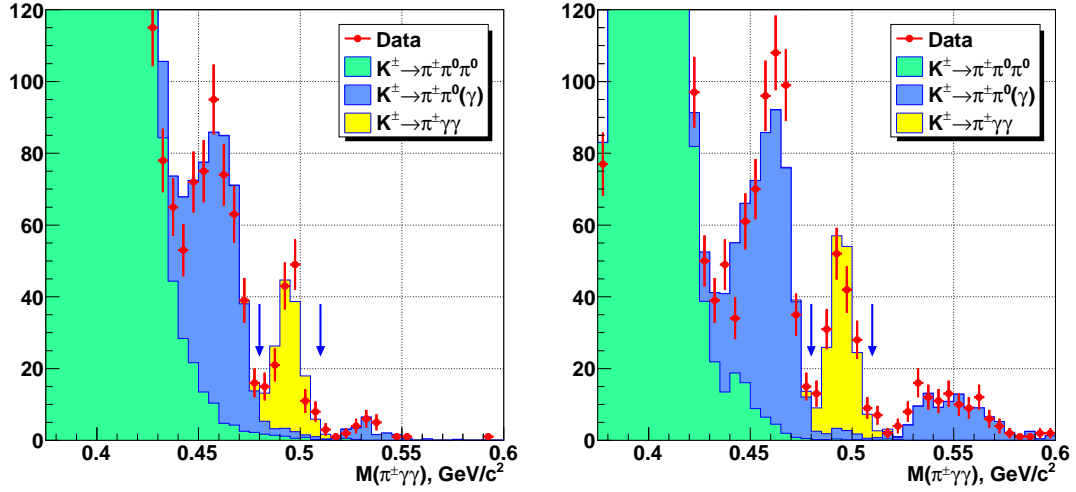


Figure 2: Distributions of $K^\pm \rightarrow \pi^\pm \gamma\gamma$ invariant mass with MC expectations for signal and backgrounds: 2004 data (left) and 2007 data (right). The signal region is indicated with arrows.

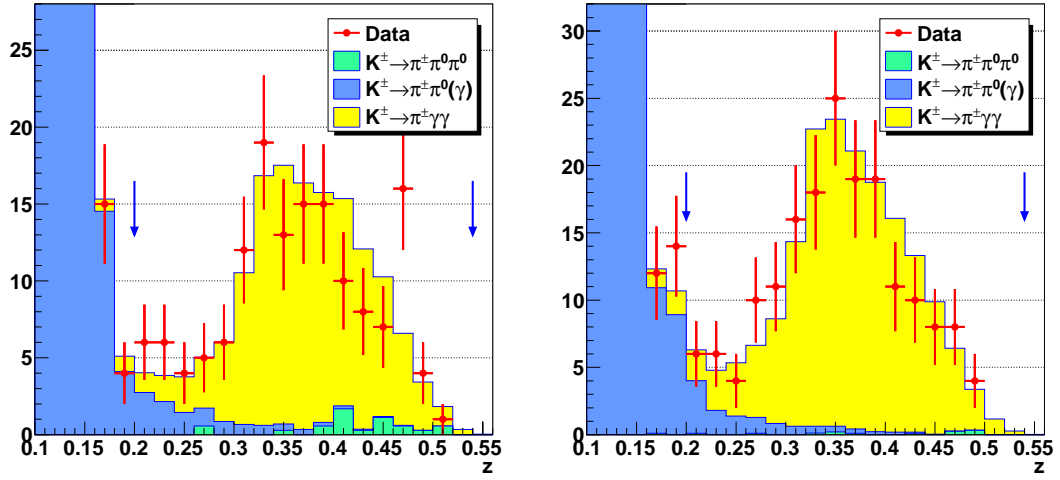


Figure 3: Distributions of $z = (m_{\gamma\gamma}/m_K)^2$ with MC expectations for signal (best fit) and backgrounds: 2004 data (left) and 2007 data (right). The estimated MC signal component corresponds to the $O(p^6)$ fit. The signal region ($0.2 < z < 0.52$) is indicated with arrows.

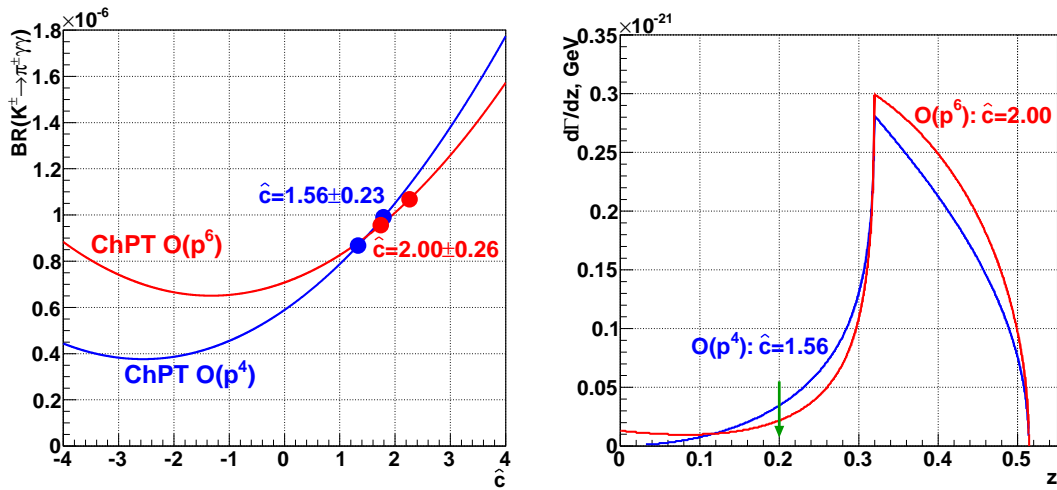


Figure 4: $K^\pm \rightarrow \pi^\pm \gamma\gamma$ branching fraction as a function of \hat{c} (left) and $K^\pm \rightarrow \pi^\pm \gamma\gamma$ differential rate in terms of $z = (m_{\gamma\gamma}/m_K)^2$ (right), for $O(p^4)$ and $O(p^6)$ parameterizations according to [4], with \hat{c} as measured from the fit to the data. The pairs of points (left) correspond to 1σ uncertainty around the combined measurement of \hat{c} .